

Fatigue failure and structural integrity analysis of a 3-inch butterfly valve shaft using finite element modelling and microstructural evaluation

K. Yuvaraj^{1*} , G. Arunkumar¹ 

¹ Department of Mechanical Engineering, Sathyabama Institute of Science and Technology, Chennai 600119, India

* Corresponding author's e-mail: Yuvaraj.kadirvelu@gmail.com

ABSTRACT

A 3-inch butterfly valve shaft failed at a water treatment plant after 50 cycles, despite having a 50000 cycles design life. To identify failure processes, a comprehensive methodology was used, which included visual inspection, microstructural analysis, and finite element analysis (FEA) to assess failure mechanisms under cyclic loading. The shaft, made of SS 316L steel with a tensile yield strength of 205 MPa and ultimate tensile strength of 515 MPa, exhibited stress concentrations in transition zones, with maximum von Mises stress reaching 506.15 MPa and total deformation of 2.6 mm. Fatigue life analysis identified regions experiencing as few as 50 cycles before failure, emphasizing the need for geometric optimization. Microstructural analysis using scanning electron microscopy (SEM) confirmed fatigue crack initiation at machining marks and propagation along grain boundaries, aligning with FEA predictions. The analysis incorporated boundary conditions, including fixed supports at flange ends, an applied moment of 27572 N.mm and an operating pressure of 1.76 Mpa. The Goodman mean stress theory was employed for fatigue life prediction, revealing von Mises stress peaks of 427.78 MPa, equivalent alternating stress of 676.84 MPa under fully reversed loading, and critical deformation of 0.081 mm. Damage analysis pinpointed failure-prone regions with a maximum damage index exceeding $1e5$, limiting the design life to approximately 1.76 million cycles in critical areas. To enhance fatigue resistance, future work proposes replacing SS 316L with XM19 steel or increasing the shaft diameter and validating its performance under simulated operational conditions and cyclic testing contains continually opening and closing the valve under test pressure to assess the leakage and operating torque as per API 609 standard. These insights are vital for improving butterfly valve durability and ensuring long-term operational reliability in industrial applications.

Keywords: fatigue behavior, butterfly valve, Goodman theory, finite element analysis, SS 316L steel, cyclic testing, failure mechanisms.

INTRODUCTION

The fatigue behavior of butterfly valves is critical to their performance and reliability, especially in process industries. A 3-inch butterfly valve failed at water treatment field after just three months, far short of its 10-year design life. The failure in the valve shaft caused leakage across the disc-seat interface, leading to wastewater contamination and an emergency shutdown. Investigations revealed that recent design modifications for cost reduction and simplified

manufacturing compromised the shaft's integrity. Replacing the double-shaft with a single-shaft design and reducing the shaft diameter at the bottom introduced stress concentration points, increasing susceptibility to fatigue failure. Cyclic pressure loads and fluctuating operational stresses accelerated fatigue damage, with stress concentration zones further compromising material endurance. The valve experienced approximately 60 pressure cycles (20 cycle per month), with peak pressure fluctuations ranging from 1.2 MPa to 1.75 MPa, significantly impacting fatigue performance.

With only a small batch of these valves installed, concerns arose about similar failures elsewhere, highlighting the need for design reassessment and structural reinforcement. Understanding how design modifications affect fatigue life is crucial for enhancing butterfly valve reliability in demanding conditions. Finite element modeling identifies stress concentration zones affecting fatigue performance in valve systems (Daradkeh and Jalali, 2023). FEA evaluates stress distribution, deformation, and fatigue life under cyclic loads, while CFD studies show the influence of geometry and material properties on stress patterns in butterfly valves (Del Toro et al., 2015). Stress hotspots in large butterfly valves are extensively analyzed through FEM (Shrivastava and Patel, 2017; Varma and Raveendra, 2016). SS 316L steel, used in this study, offers corrosion resistance and high strength but remains vulnerable to fatigue under extreme cyclic loading without stress reduction (Parmar and Mishra, 2015). The shaft failure at stress levels above 138 MPa aligns with findings that excessive torque and geometric amplifications impact fatigue performance (Naragund and Nasi, 2019). Microstructural analysis confirmed crack initiation at high-stress regions, supporting research on shaft geometry's role in failures (Salinas et al., 2020). FMEA effectively identifies failure points, emphasizing shaft geometry's role in fatigue resistance (Patil et al., 2017). Safety factors are critical for structural integrity under loads (Patil et al., 2015), while optimized designs like disc profiles and laminated seals enhance cyclic performance (Kwak et al., 2019). This study aims to investigate the fatigue behavior of a 3-inch butterfly valve shaft under cyclic and operational loads. Using Goodman mean stress theory, supported by finite element analysis (FEA) and microstructural observations, this research seeks to:

1. Evaluate stress distribution, damage, and deformation patterns under cyclic loading.
2. Identify critical zones prone to fatigue failures through microstructural analysis.
3. Propose design and material enhancements to extend the valve's operational life and ensure reliability under high-stress conditions.

Here are a few highlights of novelty of the study compared to existing research

1. In contrast to traditional research that mostly uses FEA simulations, this study uses SEM-based microstructural failure analysis to

confirm numerical results, ensuring improved fatigue prediction accuracy.

2. The influence of shaft design changes on fatigue performance is not specifically addressed in the majority of earlier research, which concentrate on generic fatigue failure root causes.
3. This study directly compares practical operational failures with design modification and identifies stress amplifications due to the changeover from a double-shaft to a single-shaft system.
4. Despite the widespread use of fatigue and FEA models, this study bridges the gap between theoretical forecasts and actual performance by using operational pressure cycles, maintenance records, and actual plant failure data.

Background and failure statement

A 3-inch butterfly valve in a water treatment plant failed after three months, far short of its 10-year design life. The failure in the valve shaft caused leakage across the disc-seat interface, leading to wastewater contamination, operational disruptions, and an emergency shutdown. An investigation revealed recent design changes aimed at reducing costs and simplifying assembly:

1. The original double-shaft design was replaced with a single-shaft was not solely cost-driven but also to reduce assembly complexity and maintenance requirements while providing improved alignment, consistent torque transfer, and operating stability.
2. The shaft diameter was reduced at the bottom section to further cut material costs.

These changes weakened the shaft, creating stress concentration points that accelerated fatigue failure under cyclic loading. Based on visual inspections, we have observed crack initiation at geometric transition zones, particularly the shaft step down area where high stress concentrations were found in FEA analysis and also no sign of corrosion-assisted fatigue are seen. With only a small batch of these valves installed, concerns arose about further failures, highlighting the need for design reassessment, fatigue analysis, and structural reinforcement. According to studies like (Naragund and Nasi, 2019), fatigue failures in stainless steel shafts under cyclic loading have been documented; fracture initiation mostly occurs in stress concentration zones, which is consistent with our findings. This study bridges that gap by evaluating a 3-inch butterfly valve shaft

using Goodman mean stress theory, finite element analysis, and microstructural observations to enhance durability and reliability under cyclic loading. In order to enhance fatigue life estimates, future research will assess alternative models such as SWT and Gerber.

MATERIALS

SS 316L steel shaft material

The SS 316L steel shaft was chosen for its corrosion resistance, durability, and cyclic loading adaptability. As an austenitic stainless steel, it withstands high stress and corrosive environments in fluid control systems. It has a tensile strength of 515 MPa, yield strength of 205 MPa, and Young’s modulus of 193 GPa. Its elasticity (Poisson’s ratio 0.28) and rigidity (shear modulus) ensure structural stability under varying loads.

$$G = \frac{E}{2(1+\nu)} = 75.4 \text{ GPa} \quad (1)$$

Fatigue characteristics were determined from stress-life (S-N) curves under fully reversed cyclic loading. The material sustained 334 MPa for 4.628 cycles and 146.45 MPa up to 7.89 million cycles, helping predict operational durability. Fatigue life analysis relies on the equation:

$$\sigma_a = \sigma_u \left(\frac{N}{N_f} \right)^b \quad (2)$$

where: σ_a is alternating stress amplitude, σ_u ultimate tensile strength, N cycles, N_f fatigue life, and b the fatigue strength exponent. Microstructural analysis using SEM identified crack initiation at stress concentrators, particularly in shaft transition zones, propagating under cyclic loading and leading to fatigue failure. This aligns with Goodman mean stress theory, which predicts failure under fully reversed loading. The Goodman mean stress correction is applied to predict fatigue life under mean stress (σ_m) and alternating stress (σ_a); Where σ_f is the fatigue limit:

$$\frac{\sigma_a}{\sigma_f} + \frac{\sigma_m}{\sigma_f} = 1 \quad (3)$$

The combination of mechanical analysis, fatigue characterization, and microstructural observations highlights the need to address stress concentrators in SS 316L shafts. These findings support geometric and material refinements to

enhance fatigue resistance and extend the service life of butterfly valve shafts.

Boundary conditions for material use

The boundary conditions in the FEA were designed to replicate real-world operational and cyclic loading scenarios for an accurate fatigue assessment of the butterfly valve. A steady-state pressure of 1.76 MPa was applied, representing the fluid force exerted on valve components during operation, ensuring precise evaluation of stress distribution and fatigue behavior:

$$F = P \cdot A \quad (4)$$

where: F is force (N), P is applied pressure (MPa), and A is the surface area (m^2). Additionally, an operational torque of 27.572 N·mm simulated forces on the shaft and disc during actuation, with shear stress defined by the moment relationship:

$$\tau = \frac{M \cdot c}{J} \quad (5)$$

where: τ is the shear stress (MPa), M is the applied moment (N·mm), c is the radius to the outer surface of the shaft (m), and J is the polar moment of inertia of the shaft’s cross-section (m^4). The von Mises stress criterion was applied to evaluate equivalent stress under combined loading conditions:

$$\sigma_v = \sqrt{\sigma_x^2 - \sigma_x \sigma_y + \sigma_y^2 + 3\tau^2} \quad (6)$$

where: σ_v is the von Mises stress (MPa), σ_x and σ_y are the normal stresses in the x- and y-directions, and τ is the shear stress. The von Mises criterion assessed yielding in SS 316L steel under multiaxial stress. Fully reversed cyclic stress modeling evaluated endurance under operational cycles. The fatigue safety factor was determined to ensure safe cyclic performance:

$$n_f = \frac{\sigma_a}{\sigma_e} \quad (7)$$

where: n_f is the safety factor, σ_a is the alternating stress amplitude (MPa), and σ_e is the endurance limit stress (MPa). The angular deflection of the valve shaft under applied torque was assessed using the deflection-torque relationship:

$$\theta = \frac{T \cdot L}{J \cdot G} \quad (8)$$

where: θ is the angular deflection (radians), T is the applied torque (N·m), L is the length of the shaft (m), J is the polar moment of inertia (m⁴), and G is the shear modulus (GPa).

The defined boundary conditions and equations accurately captured the valve’s operational and fatigue behavior. Simulating real-world conditions, FEA identified stress distribution, failure zones, and overall durability. The analysis informed design optimizations and material enhancements to improve reliability and extend valve life. Table 1 summarizes the valve’s material properties and operational parameters.

Methodology

The methodology employed in this study integrates microstructural analysis, FEA setup, and the inclusion of input parameters to comprehensively evaluate the fatigue behavior of the butterfly valve shaft.

Visual inspection

A detailed visual inspection was conducted to identify the failure characteristics and underlying causes of the butterfly valve shaft failure:

1. The shaft diameter at the failure point is visibly reduced compared to undamaged areas, indicating localized stress concentration.
2. No signs of oxidation or corrosion were observed, ruling out environmental degradation as a contributing factor.
3. The fracture surface exhibits distinct fatigue striations radiating from the crack origin, confirming cyclic loading as the primary failure mechanism.
4. A polished, shiny area was observed on the fracture surface, indicating prolonged wear due to continuous rotational motion.
5. The crack appears to have initiated at a surface defect, such as a machining mark, pitting, or sharp corner, which acted as a stress concentrator, accelerating fatigue failure.

Table 1. Specification of the butterfly valve

Parameter	Details
Size	3-inch butterfly valve
Type	Wafer
Pressure rating	1.6 MPa
Body material	ASTM A216 Grade WCB (Cast Steel, Grade B)
Seat material	Ethylene propylene (EPDM, Hardness 60 Shore A)
Trim material	Stainless steel SS 316L
Operator	Manual

6. Fretting corrosion was evident at the interface between the shaft and the mating component, suggesting its role in crack propagation and further weakening of the shaft.

These findings highlight the role of cyclic loading, stress concentration, and surface defects in premature shaft failure. Figure 1 shows the fractured SS 316L shaft post-fatigue testing, with visible deformation and discoloration near high-stress zones. These heat-affected areas correlate with fatigue crack initiation and propagation, aligning with numerical predictions identifying critical stress regions in the shaft’s transition zones.

Features of the fracture surface

The shaft failure was driven by combined torsional and bending stresses, as indicated by the fracture surface features. The origin marks the point where cracking began, characterized by the smoothest region of the surface. Adjacent to this, the fatigue zone (FZ) represents gradual crack progression under cyclic loading, with smooth surfaces and visible striations confirming repeated stress cycles. Beach marks, also known as progression or conchoidal marks, reveal variations in applied loads, highlighting dynamic loading conditions during operation. The instantaneous zone (IZ), formed when the load exceeded the material’s strength, was rough and crystalline, suggesting brittle fracture. The IZ’s small size indicates relatively low loads, but localized stress



Figure 1. Broken butterfly valve shaft during operation

concentrations likely amplified the effective stress, triggering failure.

Rotating bending and its implications

Rotating bending was evident in the asymmetric crack growth, with the bisector of the IZ deviating from the crack origin due to shaft rotation. The fracture surface also indicated the direction of rotation. The absence of progression marks suggests consistent loading, while the sharp radius at the shaft step acted as a stress concentrator, multiplying local stress. Even under low loads, this amplified stress initiated and propagated cracks. These observations underscore the need for geometric refinement to mitigate stress concentrations and enhance shaft reliability. Figure 2 shows the illustration of fatigue failure under rotating bending, highlighting stress concentration, progression marks, and origins of crack propagation.

Microstructural analysis

The analysis of the SS 316L shaft fracture surface using scanning electron microscopy (SEM) revealed fatigue cracks initiating at machining marks and propagating through grain boundaries

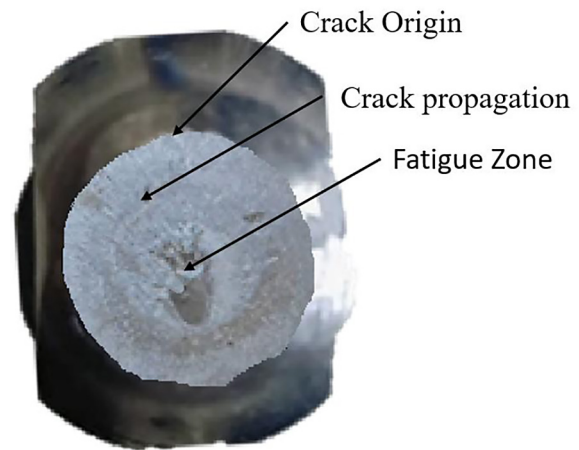


Figure 2. Fatigue failure-rotating bending

under cyclic loading. Failures were concentrated in transition zones where geometric discontinuities amplified stress. Figure 3a indicating beach marks at low magnification and striations. Figure 3b shows that striations were detected under higher magnification, demonstrating cyclic loading along with crack propagation. Figure 3c identified the last stage of fracture by the change from fatigue striations to a rougher, more disordered fracture surface.

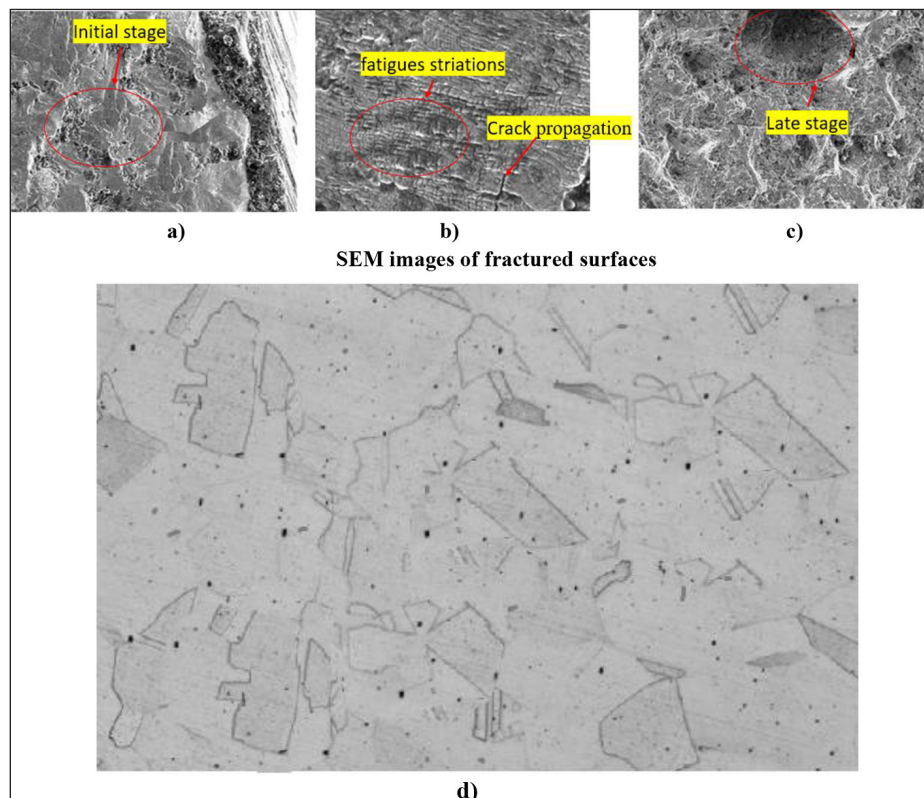


Figure 3. (a) Crack origin zone, (b) crack propagation zone, (c) fatigue zone, (d) microstructure of SS316L broken shaft

Metallographic examination identified a non-uniform hardened surface layer, often less than 1.0 mm thick, indicative of suboptimal heat treatment. The bainitic surface layer transitioned into a ferrite-pearlite structure, creating mechanical inconsistencies that increased stress concentrations. Non-metallic inclusions, such as sulfides and oxides, acted as stress concentrators, promoting crack propagation. Hardness varied significantly, with the bainitic surface measuring 478 HV compared to the softer ferritic interior at 216 HV, increasing fatigue susceptibility. Residual tensile stresses in the bainitic layer further heightened crack initiation risks. Energy Dispersive Spectroscopy (EDS) detected manganese, silicon, sulfur, and aluminum within inclusions, reducing toughness and cyclic loading resistance. These findings highlight the need for improved heat treatment methods, such as isothermal treatment or carburization, to enhance microstructural uniformity and fatigue resistance. The mean grain size of SS 316L was determined at 30 μm , with bigger grains detected in high-stress zones, perhaps lowering fatigue resistance. Inclusion analysis confirmed the existence of sulfides and oxide, which can operate as crack initiation sites under cyclic stress. There was no substantial secondary phase development, such as sigma (σ) phase or carbide precipitation, showing that fatigue failure was predominantly caused by stress amplification rather than phase transformation effects. Figure 3 (d) shows the SEM images highlight fatigue failure mechanisms such as crack propagation, surface defects, and microstructural inclusions.

Finite element model setup and boundary conditions

Finite element analysis in ANSYS 19.0 simulated the butterfly valve’s operational and cyclic

loading. The 3D model, meshed with 203,462 elements and 372,318 nodes, ensured computational accuracy and captured stress gradients in critical shaft transition zones. Based on plant installation information, the butterfly valve is permanently attached at the flange ends to prevent movement and provide exact replication in FEA as fixed supports. Figure 8 depicts boundary conditions, with a steady-state pressure of 1.76 MPa (“A”), fixed supports at both side of the flange ends (“B”), and an operational moment (actuator torque) of 27,572 N·mm (“C”) representing mechanical constraints and torque to precisely replicate the real-world plant data.

Fatigue loading was modeled as fully reversed cyclic stress using Goodman mean stress theory, predicting fatigue life by incorporating alternating and mean stresses. Figure 4(a) depicts cyclic loading, alternating between tensile and compressive states, while Figure 4(b) presents the Goodman diagram, defining safe stress regions based on ultimate strength and endurance limits. The simulation used SS 316L steel properties, including a tensile strength of 515 MPa, yield strength of 205 MPa, and shear modulus of 75.4 GPa, ensuring accuracy. CF8M stainless steel (disc, bearings) and EPDM rubber (sealing) were included to evaluate their impact. The von Mises stress criterion identified stress-prone areas under combined loading. Table 2 summarizes material properties and key input parameters for finite element analysis and fatigue evaluation.

Input parameters

The input parameters for the FEA were carefully defined to replicate the operational conditions of the butterfly valve under cyclic loading. The stress levels were analyzed with a maximum von Mises stress of 506.15 MPa, which was concentrated in

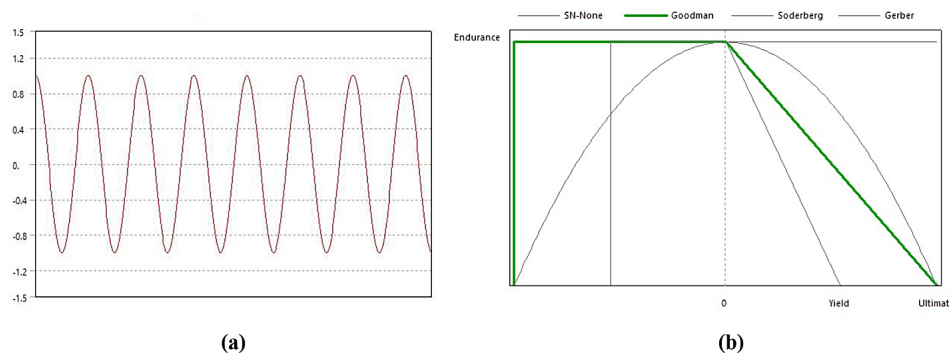


Figure 4. Fatigue analysis (a) fully reversed loading and (b) goodman theory

Table 2. FEA input parameters and material specifications

Parameter	Value	Description
Applied pressure	1.76 MPa	Represents steady-state operational fluid pressure exerted on valve components.
Applied moment	27,572 N·mm	Simulates operational torque on the shaft and disc components.
Mesh details	203,462 elements, 372,318 nodes	Ensures high-resolution stress and deformation analysis.
Shaft material	SS 316L	Austenitic stainless steel for corrosion resistance and mechanical strength.
Tensile ultimate strength	515 MPa	Maximum stress the material can withstand before failure.
Tensile yield strength	205 MPa	Stress level at which permanent deformation begins.
Young's modulus	193 GPa	Material stiffness under axial stress.
Poisson's ratio	0.28	Describes material deformation in lateral and axial directions.
Shear modulus	$G = \frac{E}{2(1+\nu)} = 75.4 \text{ GPa}$	Material rigidity under shear stress.
Sealing material	EPDM Rubber	Flexible material for sealing; Young's Modulus: 22.3 MPa, Poisson's Ratio: 0.45
Structural material	WCB Cast Steel	For valve body and flanges; Young's Modulus: 207 GPa, Poisson's Ratio: 0.29
Fatigue loading	Fully reversed cyclic stress	Modeled using Goodman mean stress theory for fatigue life prediction.
Software	ANSYS 19.0	Used for finite element modeling and simulation.
Von mises stress range	Min: 1.34 MPa, Max: 506.15 MPa	Equivalent stress distribution across the components.
Total deformation	Min: 0 mm, Max: 2.67 mm	Deformation under applied loading conditions.
Fatigue life	Up to 7.89 million cycles	Based on alternating stress of 146.45 MPa for SS 316L steel.

high-stress regions, particularly near geometric discontinuities in the shaft. Fully reversed cyclic loading was applied, correlating with the S-N curve data for Stainless Steel 316L, which provided a comprehensive fatigue life prediction under different stress amplitudes. The fatigue behavior of SS 316L, including stress amplitude vs. fatigue life data, was directly referenced from Mohammad et al. (2012) enabling precise confirmation against published experimental findings is illustrated in Table 3, which presents a range of stress amplitudes

Table 3. Fatigue behavior stainless steel 316L as per number of cycles

Load ratio (R)	Stress amplitude (MPa), σ_a	Life (cycles) $2N_f$
0.1	334.0	4628
	290.0	17340
	275.0	55478
	234.0	164938
	220.0	450447
	180.0	1033948
	160.0	4832284
	146.0	7893764

and their corresponding fatigue life (cycles). The highest stress amplitude of 334 MPa led to failure within 4,628 cycles, while a lower stress amplitude of 146 MPa allowed for a significantly longer fatigue life of 7,893,764 cycles. This data was directly used in FEA to model fatigue loading conditions and assess the material's performance under repeated cyclic stress.

The Goodman mean stress theory was employed to evaluate the fatigue response of SS 316L, particularly in areas with high-stress concentrations such as the shaft transition zones. By incorporating both alternating stress amplitude and mean stress, this approach accurately predicted fatigue life and identified regions susceptible to early failure. The S-N curve (Figure 5) visually depicts the relationship between stress amplitude and fatigue life, emphasizing the inverse correlation where higher stress levels significantly reduce material lifespan. The curve follows the power law equation $y = ax^b$, which provides a mathematical model for predicting fatigue performance under various loading conditions. This data plays a crucial role in FEA simulations, enabling a more precise fatigue analysis and guiding

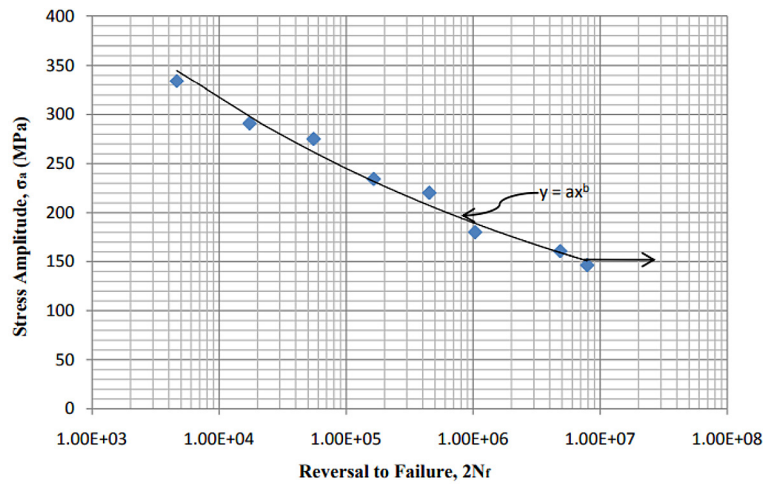


Figure 5. S-N curve of stainless steel 316L (Source: 11. Mohammad et al., 2012)

design optimizations for improved durability and reliability of the butterfly valve shaft.

Finite element analysis and structural evaluation

Finite element analysis (FEA) was performed to evaluate the stress distribution within the butterfly valve assembly under operational and fatigue loading conditions.

Stress analysis

The von Mises stress criterion identified maximum equivalent stress regions. Figure 6 illustrates the 3-inch butterfly valve's geometry, defining

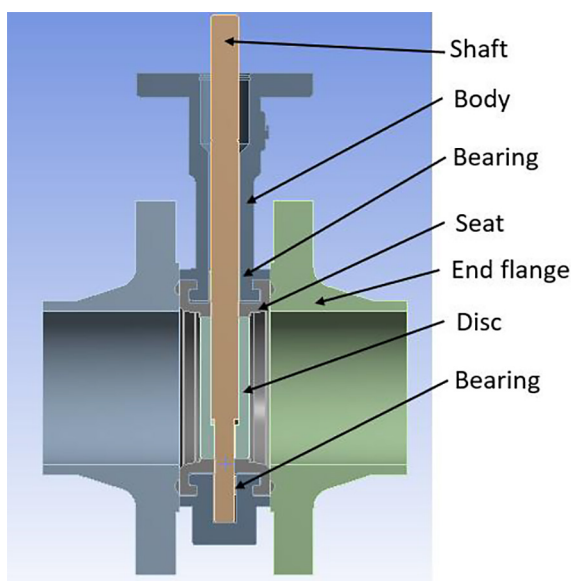


Figure 6. Cross-sectional geometry of the butterfly valve assembly

key components like the shaft, disc, and housing. The meshed model, with 203,462 elements and 372,318 nodes, ensures high-resolution stress analysis. Fine meshing in critical regions, particularly the shaft's transition zones, accurately captures stress gradients essential for fatigue evaluation. Figure 7 highlights the meshed 3D geometry, detailing discretized elements crucial for analyzing stress distribution in critical areas like the shaft and disc. Figure 8 depicts boundary conditions, with a steady-state pressure of 1.76 MPa ("A"), fixed supports at both side of the flange ends ("B"), and an operational moment of 27,572 N·mm ("C") representing mechanical constraints and torque to precisely replicate the real-world plant data. Figure 9(a) shows von Mises stress distribution in the shaft, ranging from 1.339e-5 MPa to 427.78 MPa. High-stress zones near transition areas indicate potential failure points, highlighting the need for material optimization or geometric adjustments.

Equivalent alternating stress distribution

Figure 9(b) presents the equivalent alternating stress in the shaft, peaking at 676.84 MPa, with the highest concentrations at sharp geometric transitions, aligning with observed failure zones. Figure 10 shows deformation analysis, indicating a maximum displacement of 0.081279 mm, primarily near loading points, while minimal displacement in low-stress regions ensures structural stability.

Fatigue life and safety factor

The fatigue life analysis utilized stress-life (S-N) curve data for SS 316L steel, with fully

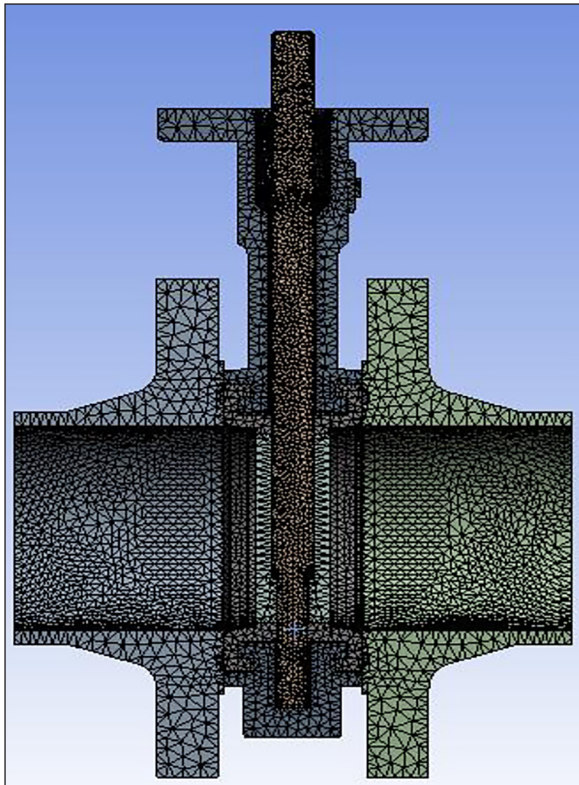


Figure 7. Geometry and mesh model of the valve assembly

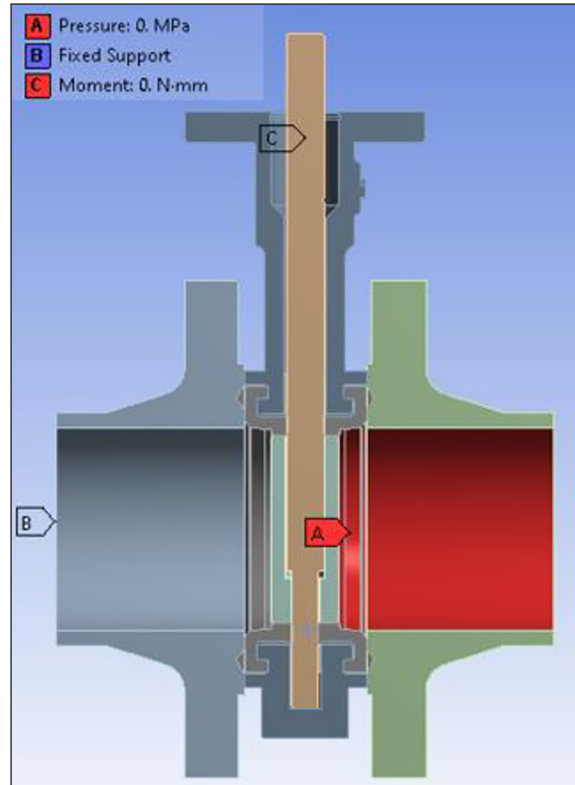


Figure 8. Boundary condition of valve assembly

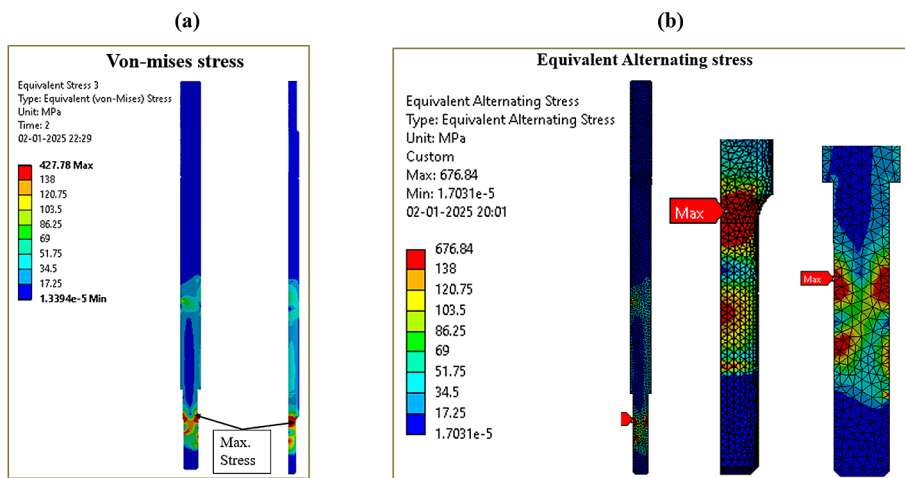


Figure 9. Stress distribution: (a) Von Mises stress distribution in butterfly valve shaft (b)

reversed cyclic loading modeled through the Goodman mean stress theory to assess fatigue performance. The study correlated alternating stress amplitudes with failure cycles, enabling safety factor evaluation. Time-dependent variations in operational pressure and moment were analyzed, as shown in Table 4. The operational pressure ramped to 1.76 MPa, while torque increased to 27,572 N·mm within 2 seconds, accurately simulating real-world loading

conditions and mechanical stresses experienced during valve actuation.

Figure 11a shows the fatigue life distribution of the butterfly valve shaft under cyclic loading, with a maximum life of 7.89 million cycles and critical zones as low as 50 cycles. These stress concentrators near geometric transitions highlight the need for design improvements to prevent premature failure. Figure 11b illustrates the safety factor distribution,

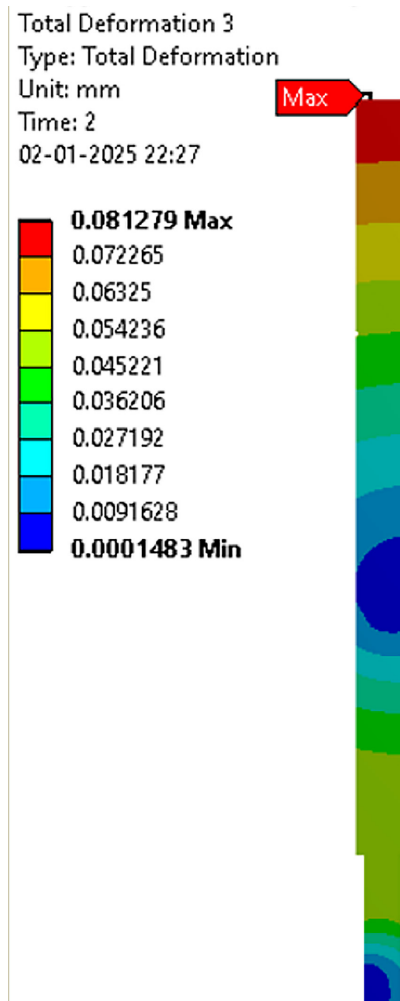


Figure 10. Total deformation profile

ranging from 15 to a critical minimum of 0.21637. Low safety factor regions, marked in red, correspond to high-stress areas prone to failure, emphasizing the necessity of structural optimization for improved valve reliability.

Damage analysis

Critical damage regions were identified by correlating stress distribution with observed failure modes. SEM micrographs confirmed crack initiation in high-stress zones. Figure 12 illustrates damage distribution across the shaft, with values ranging from 126.68 to over 1×1032 . Red-marked areas indicate severe damage, mainly at geometric transitions and stress concentrators. Addressing these zones is crucial to mitigating damage progression and improving fatigue resistance in the valve shaft.

Table 4. Pressure variation & moment variation during simulation

Load ratio (R)	Stress amplitude (MPa), σ_a	Life (cycles) $2N_f$
0.1	334.0	4628
	290.0	17340
	275.0	55478
	234.0	164938
	220.0	450447
	180.0	1033948
	160.0	4832284
	146.0	7893764

RESULTS AND DISCUSSION

The analysis highlighted key insights into the fatigue behavior and reliability of the butterfly valve shaft. Fatigue failure originated in high-stress concentration zones, particularly in geometric transitions, as confirmed by SEM imaging, which revealed crack initiation and propagation at the microstructural level. These findings aligned with finite element analysis, which identified the same critical failure zones. Cyclic loading, modeled as fully reversed stress using the Goodman mean stress theory, demonstrated the influence of alternating and mean stresses on fatigue failure. The Goodman diagram outlined critical loading scenarios where the design neared or exceeded safety limits, emphasizing the need for geometric optimization and material enhancements to reduce stress concentrations. Table 5 consolidates results across the valve assembly, showing a maximum equivalent stress of 506.15 MPa and total deformation of 2.67 mm, highlighting areas needing reinforcement. Safety factors below 1 in certain regions indicate a risk of material failure. The observed fatigue failure at 50 cycles is also associated with high von Mises stress, which exceeded the allowable stress limit, resulting in early crack initiation. This confirms that the failure was stress-related and also amplification effects. The time-dependent analysis revealed increasing stress and deformation, peaking at 2 seconds, reflecting the dynamic structural response under cyclic loading.

The maximum operational stress reached 506.15 MPa, exceeding the material’s yield strength and accelerating fatigue damage, as verified by SEM observations. This underscores the need for improved material properties or

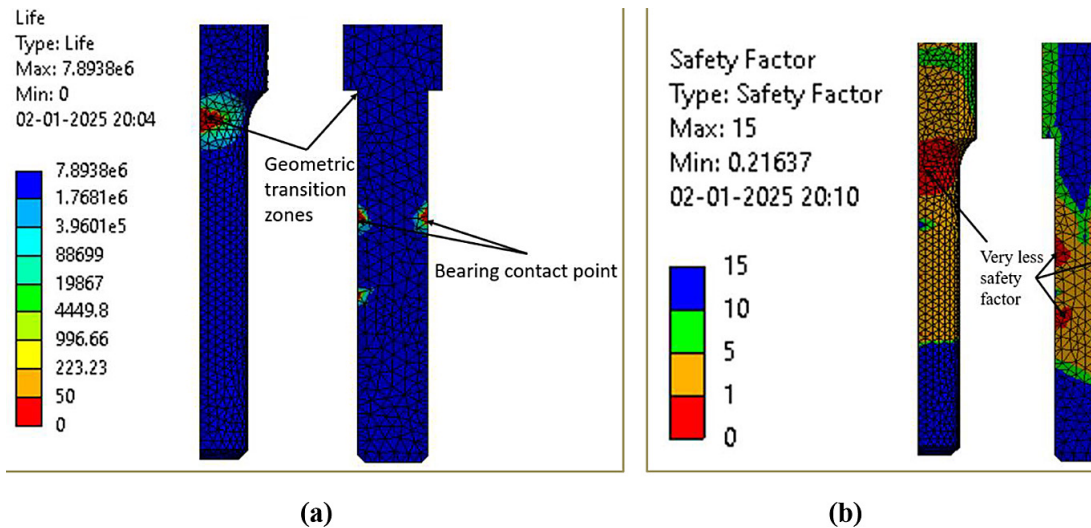


Figure 11. Distribution in butterfly valve shaft: (a) fFatigue life, (b) safety factor

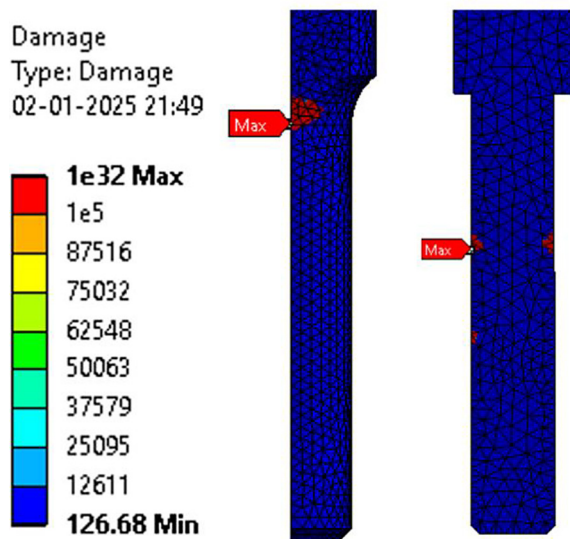


Figure 12. Damage distribution in butterfly valve shaft

optimized loading configurations to reduce stress and extend the shaft’s lifespan.

To further investigate fatigue behavior, fracture mechanics evaluation became taken into consideration because of found crack growth. The envisioned stress intensity factor and crack propagation rate which indicate that failure was caused by cyclic crack growth, which was consistent with the Goodman mean stress theory and S-N curve results. Microstructural analysis confirmed that fatigue resistance is strongly influenced by material properties and geometric features, with SEM images showing cracks concentrated in high-stress zones. Localized plastic deformation and stress risers further amplified fatigue damage, leading to premature failure. Enhancing fatigue resistance requires material refinement and design modifications to mitigate

Table 5. Consolidated FEA results for deformation, stress, and fatigue life

Parameter	Minimum	Maximum	Average	Time [s]
Total deformation [mm]	0.0003143	2.6777	0.13962	2
	0.0039314	2.6777	1.0844	1
Equivalent stress [mPa]	7.0702×10^{-15}	506.15	14.584	2
	2.4313×10^{-14}	116.71	8.0242	1
Equivalent alternating stress [mPa]	9.7933×10^{-5}	196.91	13.991	2
	7.1638×10^{-4}	89.652	12.251	1
Maximum shear stress [mPa]	3.9637×10^{-15}	238.21	10.01	2
	1.3922×10^{-14}	19.297	1.302	1
Fatigue life [cycles]	50	7.89×10^6	-	-
Safety factor	0.21637	15	-	-

stress concentrations and improve durability. Both numerical analysis and experimental results revealed that fatigue failure occurred at geometric transition zones with the highest stress concentrations. The observed crack initiation and propagation patterns (verified via SEM imaging) corresponded to places where FEA projected maximal von Mises stress (~506.15 MPa) and fatigue failure within low cycle ranges (~50 cycles in critical zones). In addition to suggesting shaft material to XM19 for its higher yield strength (~690 MPa vs. 205 MPa for SS 316L) and improved fatigue resistance. Maximum equivalent stress will be reduced below the endurance limit and greatly enhancing fatigue life. The fatigue life in high-stress areas will be increased by nearly 3×, lowering the probability of early crack start.

The Fatigue tool used in the analysis is listed in Table 6 that details the parameters for evaluating fatigue behavior under fully reversed loading.

Table 6. Fatigue tool

Object name	Fatigue tool
State	Solved
Domain	
Domain type	Time
Materials	
Fatigue strength factor (kf)	1
Loading	
Type	Fully reversed
Scale factor	1
Definition	
Display time	End time
Options	
Analysis type	Stress life
Mean stress theory	Goodman
Stress component	Abs max principal
Life units	
Units name	Cycles
1 cycle is equal to	1 cycle

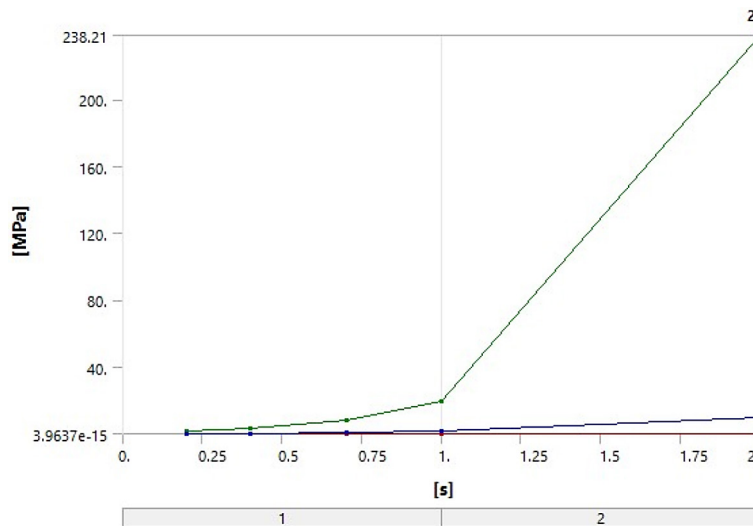


Figure 13. Maximum shear stress

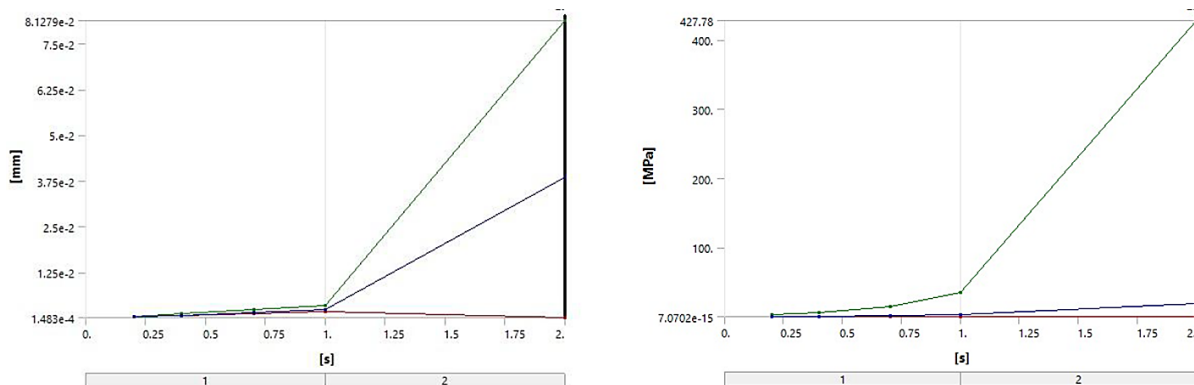


Figure 14. Total deformation 3 and its equivalent stress 3

Defined as “Solved,” the analysis operates in a time-dependent domain with a fatigue strength factor (Kf) of 1. The “Stress Life” analysis type incorporates the Goodman mean stress theory to assess fatigue life using absolute maximum principal stress. The results, displayed at the end time, are recorded in cycles, with each cycle equating to 1. Figure 13 focuses on maximum shear stress distribution, emphasizing areas vulnerable to shear-induced failure. Figure 14 presents a third iteration of deformation and stress analysis, reinforcing previous findings and providing deeper insights into structural behavior and stress propagation in the valve assembly under operational conditions.

CONCLUSIONS

The analysis of the 3-inch butterfly valve shaft using finite element modeling, Goodman mean stress theory, and experimental observations identified critical stress zones in geometric transition areas. Maximum equivalent stress reached 506.15 MPa, with a total deformation of 2.6 mm under operational conditions. Fatigue life distribution revealed regions with as few as 50 cycles, highlighting the need for geometric optimization. Safety factor values below 1.0 confirmed a high risk of failure, aligning with SEM observations of crack initiation and propagation at stress concentrators. Damage distribution analysis validated FEA predictions, with severe damage indices in transition zones. The Goodman diagram identified critical loading conditions requiring design improvements. Recommendations include material refinement for enhanced fatigue strength, geometric modifications to reduce stress concentrations, and periodic monitoring for early fatigue detection, ensuring the structural integrity and longevity of butterfly valves under cyclic loading. As a part of further work we plan to explore the comparative validation of alternative fatigue models (e.g., Smith-Watson-Topper or Gerber). By comparing these models to our present Goodman-based method, we seek to improve the accuracy of fatigue life forecasts and provide better design recommendations for butterfly valve shafts.

To further enhance the durability and reliability of the butterfly valve shaft, future investigations will focus on replacing the current SS 316L material with XM19, which offers superior mechanical strength and corrosion resistance. Finite element analysis will be employed to simulate operational

conditions and assess the fatigue behavior of the upgraded material under cyclic loading. Additionally, experimental cyclic tests will be conducted to validate the performance of the XM19 shaft and compare it with the existing design. This study will aim to optimize fatigue life, reduce stress concentrations, and ensure long-term operational integrity in demanding industrial applications. Field experiments will be advised to evaluate real-world performance and ensure that the optimized design effectively reduces failure risk. These techniques are intended to lengthen fatigue life, reduce stress concentrations, and improve the long-term structural integrity of butterfly valves in demanding industrial applications.

REFERENCES

1. Daradkeh, A.M., & Jalali, H.H. Finite element modeling aspects of buried large diameter steel pipe – butterfly valve interaction. *Modelling*, 2023; 4(4), 548–566.
2. Del Toro, A., Johnson, M.C., & Spall, R.E. Computational fluid dynamics investigation of butterfly valve performance factors. *Journal-American Water Works Association*, 2015; 107(5), E243–E254.
3. Kwak, H.S., Seong, H., Brilianto, R.M. and Kim, C. Design of laminated seal for triple offset butterfly valve (350 °C) used in combined cycle power plants. *Applied Sciences*, 2019; 9(15), 3095. <https://doi.org/10.3390/app9153095>
4. Lee, M.H., & Son, I.S. (2020). Structural stability of high-temperature butterfly valve using interaction analysis. *Journal of the Korean Society of Industry Convergence*, 23(6–1), 881–888.
5. Li, S., Zheng, M., Wang, Y., Yang, L., & Ma, T. Multi-objective optimization design of double resilient groove metal seat for ball valve in liquid hydrogen receiving stations. *Journal of the Brazilian Society of Mechanical Sciences and Engineering*, 2024; 46(1), 34.
6. Lin, Z., Yin, D., Tao, J., Li, Y., Sun, J., & Zhu, Z. Effect of shaft diameter on the hydrodynamic torque of butterfly valve disk. *Journal of Fluids Engineering*, 2020; 142(11), 111202.
7. Mohammad, K.A., Ali, A., Sahari, B.B., & Abdullah, S. Fatigue behavior of austenitic type 316L stainless steel. In *IOP conference series: materials science and engineering 2012*, September; 36(1), 012012. IOP Publishing.
8. Naragund, P.S., & Nasi, V.B. CFD method of prediction and validation of operating torque for butterfly valves with various disc profiles. *Journal of*

- Innovation in Mechanical Engineering, 2019; 2(1), 1–5.
9. Parmar, K.S., & Mishra, Y. Structural design and FEM analysis of large butterfly valve: A review. *International Journal of Engineering and Technical Research (IJETR)* 2015.
 10. Patil, R.B., Jadhav, V.S., Waghmode, L.Y., Kothavale, B.S., & Center, V. Failure mode and effect analysis (FMEA) of manually and electrically operated butterfly valve. *Pumps valves and systems*, 2017; 8(4), 8–18.
 11. Patil, R.B., Waghmode, L.Y., Jadhav, V.D., & Kothavale, B.S. Failure mode effect and criticality analysis (FMECA) of manually and electrically operated butterfly valve. In: 2nd SRESA National Conference on 'Reliability and Safety Engineering (NCRS'15). 2015; 6.
 12. Salinas, M.A., Green, J.W., & Tran, K. Revising the city of Houston's standard butterfly valve detail for large diameter butterfly valves. In *Pipelines 2020*; 221–228. Reston, VA: American Society of Civil Engineers.
 13. Shrivastava, A., & Patel, A. Structural design & fem analysis of large butterfly valve. *International Research Journal of Engineering & Applied Sciences, IRJEAS*, 2017; 2322–0821.
 14. Varma, V. L., & Raveendra, A. Structural design and FEM analysis of butterfly valve. *International Journal of Research in Engineering and Applied Sciences*, 2016; 1(6), 56–63.
 15. Yuvaraj, K. & Arunkumar, G. Simulation and validation of the effect of hydrostatic and non-hydrostatic pressure on contact pressure in a resilient seat butterfly valve. *Materials Research Express*. 2025. 12. 10.1088/2053-1591/ada877.
 16. Haimin, W., Feng, H., Xiangshuai, K. and Si, C. Pressure fluctuation of steam on the disc in a triple eccentric butterfly valve. *SN Applied Sciences*, 2020; 2(7), 1–10. <https://doi.org/10.1007/s42452-020-2992-9>
 17. Zhang, J., Yin, W., Wang, X., Zheng, S., Pan, L., & Zhai, F. Flow field torque analysis and valve plate optimization of butterfly anti-stick bleed valve. *Flow Measurement and Instrumentation*, 2024; 100, 102685.
 18. Yuvaraj, K. & Kumar, G. Study on characteristics and performance of butterfly valve using numerical methods - A review. *AIP Conference Proceedings*. 2022; 2460, 030004. 10.1063/5.0095622.
 19. Kan, B. and Chen, L. Numerical analysis of flow field in link rod butterfly valve for high-temperature steam. *Journal of the Brazilian Society of Mechanical Sciences and Engineering*, 2020; 42(4), 1–11. <https://doi.org/10.1007/s40430-020-02294-6>
 20. Kwak, H.S., Seong, H., Brilianto, R.M. and Kim, C. Design of laminated seal for triple offset butterfly valve (350 °C) used in combined cycle power plants. *Applied Sciences*, 2019; 9(15), 3095. <https://doi.org/10.3390/app9153095>